NUCLEAR INSTRUMENTS AND METHODS 127 (1975) 361–370; © NORTH-HOLLAND PUBLISHING CO.

DESIGN FOR A CONVENTIONAL HIGH-RESOLUTION NEUTRON POWDER DIFFRACTOMETER

A. W. HEWAT

Institut Laue–Langevin, B.P. N° 156, 38042-Grenoble Cédex, France

Received 14 April 1975

The design considerations for a conventional neutron powder diffractometer are reconsidered. We find that the resolution can be improved to the limits imposed by the powder particle size, while the effective intensity can at the same time be increased by using multiple counters with the correct combination of soller divergences, monochromator mosaic spread, and take-off angle. With the profile technique for data analysis, this high-resolution diffractometer should permit the refinement of nuclear and magnetic structures having unit cells of up to 3500 Å^3 volume.

1. Introduction

A neutron powder diffractometer is not required to separate all of the diffraction lines, since complex patterns containing many overlapping lines can be analysed with the profile-refinement technique[1]). Nevertheless, increased resolution will increase the amount of information in the profile and permit the solution of larger and more complicated structures[2]). The profile technique depends, though, on a precise knowledge of the line shape, and it is not permissable to obtain increased resolution at the expense of precision or intensity.

This makes it difficult to simply copy the focussing techniques used in X-ray cameras. The line profile for a conventional neutron powder diffractometer can be described as a very simple function of the scattering angle, because the diffractometer geometry is so simple: the sample is a cylinder of low absorption, the incident radiation is selected from a white beam by a monochromator having an effectively Gaussian mosaic spread, and the line shape, being a convolution of a number of nearly Gaussian distributions, approaches even more closely the ideal Gaussian shape. This can be compared to the focussing X-ray camera where the sample is an extended plate: even without the problems of absorption and α_1, α_2 radiation components, this geometry makes for a more complicated line profile[3]).

Neither can we accept a reduction in the line intensity. In fact we need an increase in intensity, since the higher resolution will permit the determination of larger crystal structures for which the average Bragg intensity will go down with increasing cell volume.

We propose then to retain the simple geometry of the conventional neutron powder diffractometer, and to calculate the ultimate resolution that can be obtained in a powder pattern. We will then show that the diffractometer can be designed to provide the intensity needed for the largest structures which can be examined with this improved resolution, i.e. unit cells of up to 3500 Å^3 volume. This calls for an improvement over the best existing diffractometers by a factor of five in resolution and at least forty in effective intensity.

2. Resolution and intensity requirements

The resolution of a powder diffractometer is ultimately limited by the particle-size effect[4]), which produces a broadening $\delta(2\theta)$ of the full width at half height, $A_{\frac{1}{2}}$, of the diffraction lines. This broadening is proportional to the ratio of the wavelength λ to the effective particle size D:

$$\delta(2\theta) = \frac{K}{\cos\theta}\left(\frac{\lambda}{D}\right). \tag{1}$$

$K \simeq 1$ is a constant depending on the particle shape and the way in which D is defined. This equation is obtained simply by differentiating the length $k = 2\lambda^{-1}\sin\theta$ of the scattering vector with respect to θ, and remembering the size in reciprocal space of the Bragg spot $\delta k \simeq D^{-1}$. Of course, the effective particle size D is not equal to the size of the powder grains: there would then be no particle-size limitation, because the large size of the sample (~ 10 cm^3) permits the use of relatively course powders. D is, instead, the size of the perfect crystallites which make up a mosaic crystal grain, or at least this mosaic model serves as a convenient link between the particle-size effect and the primary extinction effect.

The fraction ∂q of the amplitude scattered into the reflexion (h,k,l) per thickness $\partial\tau$ of a perfect crystallite is proportional to the scattering amplitude per unit volume F_{hkl}/v_c [5]):

$$\frac{\partial q}{\partial \tau} = \left(\frac{\lambda}{\sin\theta}\right)\frac{F_{hkl}}{v_c}. \quad (2)$$

F_{hkl} is the structure factor, and v_c the unit cell volume. The maximum value of F_{hkl} occurs if all the atoms add in phase: then we can take the ratio of the average atomic scattering length $b \simeq 0.66\times10^{-4}$ Å to the volume per atom $v_a \gtrsim 10$ Å^3 (e.g. solid deuterated CH_3, having one of the highest values of F_{hkl}/v_c). With $\lambda = 1.5$ Å and $\theta = 30°$ we have:

$$\partial q/\partial\tau \leq 2\times10^{-5}\ \text{Å}. \quad (3)$$

This means that the amplitude of the incident beam is reduced by no more than 2% after passing through 1000 Å of perfect crystallite, even when the strongest possible reflexion is excited. For complex structures this thickness will be larger, because there is no reflexion for which all atoms add perfectly in phase.

The fact that primary extinction in a mosaic crystal is often a larger effect than a 2% reduction in the amplitude of the strongest reflexion means that the perfect crystallites are usually larger than 1000 Å. Even for powders, this conclusion is supported by X-ray measurements of the particle size[4]). 1000 Å is, however, the correct order of magnitude, and eq. (1) with $\lambda = 1.5$ Å and $\theta = 30°$ then yields a particle-size broadening of $\delta(2\theta)\sim0.1°$. This seems to be about the limit of resolution that we can expect from a neutron powder diffractometer.

It is not, however, necessary to have such good resolution for all scattering angles. We must match the instrument resolution function to the required resolution function if we are not to needlessly sacrifice intensity. To find the required resolution function we obtain the derivative $\partial\theta/\partial p$ of the Bragg equation:

$$\frac{2d\sin\theta}{\lambda} = p^{\frac{1}{2}} \quad (4)$$

with respect to $p = h^2+k^2+l^2$ for a cubic cell of dimension d. Then the separation between adjacent peaks ($\Delta p = 1$) is:

$$\Delta(2\theta) = 2\Delta(\theta) = \left(\frac{\lambda}{2d}\right)^2\frac{2}{\sin 2\theta}. \quad (5)$$

This is symmetrical about the minimum of $2\theta = 90°$ (fig. 1). If we choose this minimum to be 0.1°, then with a wavelength of 1.5 Å we can just resolve adjacent lines for a cubic structure with $d = 24$ Å [6]).

In practice we expect the maximum cell dimensions for which lower symmetry structures can be successfully refined will be about half this figure i.e. 15 Å, or twice the dimensions of the $NH_4H_2PO_4$ cell which was refined on the PANDA diffractometer with a resolution of 0.5° [2]). On doubling the cell dimensions, the number of reflexions is increased by a factor of eight, for which the improvement in resolution from 0.5° to 0.1° will largely compensate. A 15 Å cell limit, or a volume limit of 3500 Å^3, will cover almost all of the problems of interest for powder refinement, as well as a large proportion of those which are at present studied with single-crystal neutron diffraction.

Doubling the cell dimensions will also reduce the average line intensity by a factor of eight. Furthermore, as we shall see in section 5, improving the resolution from 0.5° to 0.1° results in a loss of a factor of 25 in the line intensity, or 5 in the peak height. The effective neutron flux for the high-resolution diffractometer will then have to be between 40 and 200 times that of the Harwell machine under similar conditions of high resolution. This large factor can be achieved by the use of multiple counters on the high-flux ILL reactor: the Harwell machine used for the $NH_4H_2PO_4$ work had only one counter and about 10% of the reactor flux available at Grenoble.

3. Monochromator take-off angle

The full width at half height $A_{\frac{1}{2}}$ for the powder peaks[7]):

$$A_{\frac{1}{2}}^2 = U\tan^2\theta + V\tan\theta + W, \quad (6)$$

has a minimum at $\tan\theta = -V/2U$. The integrated line intensity L is also given here for reference.

$$U = \frac{4(\alpha_1^2\alpha_2^2+\alpha_1^2\beta^2+\alpha_2^2\beta^2)}{\tan^2\theta_M(\alpha_1^2+\alpha_2^2+4\beta^2)}, \quad (7a)$$

$$V = \frac{-4\alpha_2^2(\alpha_1^2+2\beta^2)}{\tan\theta_M(\alpha_1^2+\alpha_2^2+4\beta^2)}, \quad (7b)$$

$$W = \frac{\alpha_1^2\alpha_2^2+\alpha_1^2\alpha_3^2+\alpha_2^2\alpha_3^2+4\beta^2(\alpha_2^2+\alpha_3^2)}{(\alpha_1^2+\alpha_2^2+4\beta^2)}, \quad (7c)$$

$$L = \frac{\alpha_1\alpha_2\alpha_3\beta}{(\alpha_1^2+\alpha_2^2+4\beta^2)^{\frac{1}{2}}}. \quad (7d)$$

Then the minimum in $A_{\frac{1}{2}}$ occurs at:

$$\tan\theta = -\frac{V}{2U} = \frac{4\alpha_2^2(\alpha_1^2+2\beta)}{8(\alpha_1^2\alpha_2^2+\alpha_1^2\beta^2+\alpha_2^2\beta^2)}\tan\theta_M \simeq \tan\theta_M \quad (8)$$

since $(\alpha_1 \ll \beta, \alpha_2)$ is required for the best resolution and intensity (section 5). This is the well-known parallel

focussing condition $\theta = \theta_M$, and is not strongly dependent on the choice of collimator divergences and monochromator mosaic spread.

For a good match between the resolution function for the diffractometer [eq. (6)] and the resolution function required to separate adjacent peaks [eq. (5)], we must then choose the monochromator take-off angle $2\theta_M \sim 90°$. This is considerably larger than that available on most existing powder diffractometers, but in practice it is a good idea to choose an even larger take-off angle[8]), since $A_{\frac{1}{2}}$ increases more rapidly than does $A(2\theta)$ at high scattering angles. Fig. 1 shows how the matching to the required resolution function may be achieved with $2\theta_M \simeq 120°$ [6]).

4. Focussing in reciprocal space

It is useful to investigate the parallel focussing geometry in reciprocal space. The left-hand section of fig. 2 represents the reciprocal lattice for the monochromator, with the mosaic spread drawn as an arc around the origin. If we suppose that the direction of the incident beam IO is well defined by tight collimation α_1, then the monochromator selects a particular wavelength for each diffracted direction within a range of directions 2β. For maximum intensity, the collimator α_2 between the monochromator and the sample should accept just this range of wavelengths and directions i.e. $\alpha_2 = 2\beta$. Larger values for α_2 simply increase the background, but smaller values can be used to limit the effective mosaic spread of the monochromator when maximum intensity is not required.

The right-hand section of fig. 2 shows the reciprocal lattice for the powder sample, where the usual Bragg points have become spheres centred on the origin. The rays IM and JN from the monochromator have been redrawn as I'M' and J'N' incident on the sample. If the direction of the scattered neutrons entering the counter is also well defined by tight collimation α_3, then the Bragg equation can be satisfied for only a small arc which is an image of the mosaic spread of the collimator. When the counter direction is varied, this arc cuts through the Bragg sphere at a tangent. It is this tangetial interception of the Bragg sphere by the image of the monochromator mosaic spread that yields a sharp peak in the diffraction pattern as all of the rays of different wavelength are simultaneously reflected. The width of this focussed peak depends on how precisely the directions of the incident and diffracted beams are defined: in fact, this peak will be just the convolution of the transmission functions for the collimators α_1 and α_3, and will not depend on α_2 or β. However, the line intensity will be a function of β if $\alpha_2 \geqslant 2\beta$, since it is proportional to the area of interception. Good intensity as well as good resolution will therefore be obtained if we choose $\alpha_2 = 2\beta > \alpha_1 = \alpha_3$. When $\theta \neq \theta_M$, the interception with the Bragg sphere is no longer tangential, and the peak width increases as we go away from the focussing geometry. Since the rate of increase will be proportional to β, this defocussing effect means that β must be limited if good resolution is to be obtained for a range of scattering angles.

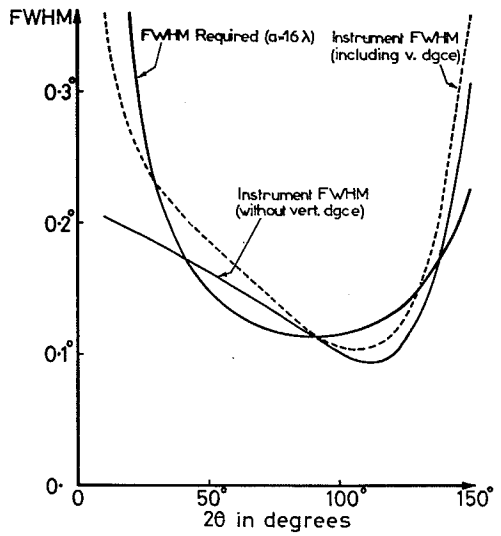

Fig. 1. Full width at half height for a high-resolution ($\alpha = 0.1°/\sqrt{2}$) conventional powder diffractometer with $\alpha_1 = \alpha_3 = \alpha$, $\beta = 2\alpha$ and $\alpha_2 = 2\beta$. These collimators, α_i, and monochromator mosaic spread, β, have been chosen so that the diffractometer resolution (solid line) matches that required to resolve adjacent lines for an hypothetical cubic crystal of lattice dimension $a = 24$ Å (points), with maximum line intensity.

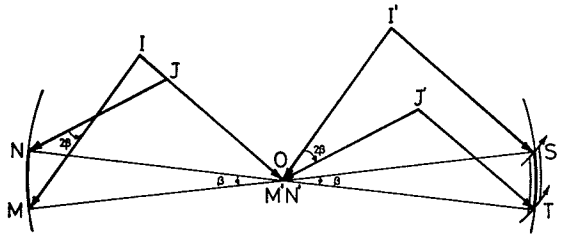

Fig. 2. Reciprocal space focussing for parallel geometry in which the collimators α_1 and α_3 are parallel, i.e. the counter collects I'S and J'T parallel to IO incident on the monochromator. Then the Ewald sphere ST, which is an image of the arc MN representing the monochromator mosaic spread β, cuts through the powder diffraction sphere at a tangent. The line shape is independent of β and α_2, being simply the convolution of the triangular transmission functions for α_1 and $\alpha_3 = \alpha_1$.

5. Collimator and monochromator combinations

Having thus found the purpose of the different collimators, we can simplify eqs. (7) and obtain more precise information on the best combination of α_1, α_2, α_3, and β.

If $\alpha_2 = 2\beta > \alpha_1 \sim \alpha_3$, then:

$$U \simeq (2.5\alpha_1^2 + 2\beta^2) \tan^{-2}\theta_M, \tag{9a}$$

$$V \simeq -(2\alpha_1^2 + 4\beta^2) \tan^{-1}\theta_M, \tag{9b}$$

$$W \simeq 0.5\alpha_1^2 + 2\beta^2 + \alpha_3^2, \tag{9c}$$

$$L \simeq \frac{1}{\sqrt{2}}\alpha_1\alpha_2\beta. \tag{9d}$$

We need only consider the scattering angles $\theta = 0°$, θ_M and $\tan\theta/\tan\theta_M = 2$ ($2\theta \simeq 150°$ if $2\theta_M = 120°$).

$$\theta = 0°, \qquad A_{\frac{1}{2}}^2 \simeq 0.5\alpha_1^2 + \alpha_3^2 + 2\beta^2, \tag{10a}$$

$$\theta = \theta_M, \qquad A_{\frac{1}{2}}^2 = (\alpha_1^2 + \alpha_3^2) - \frac{\alpha_1^4}{\alpha_1^2 + \alpha_2^2 + 4\beta^2}$$

$$\simeq \alpha_1^2 + \alpha_3^2, \tag{10b}$$

$$\frac{\tan\theta}{\tan\theta_M} = 2, \quad A_{\frac{1}{2}}^2 \simeq 6.5\alpha_1^2 + \alpha_3^2 + 2\beta^2. \tag{10c}$$

Eq. (10b) for focussing is true in more general circumstances, and represents the convolution of α_1 and α_3. Eqs. (9a) and (10b) show that the best intensity and resolution are obtained with $\alpha_1 = \alpha_3 = \alpha$ say, and eq. (9d) also shows that the line intensity is proportional to β, which is limited because eqs. (10a) and (10c) show that the half width rises to $A_{\frac{1}{2}} \gtrsim \sqrt{2}\beta$ away from the focussing geometry. Eq. (10c) indicates that $\beta \sim 2\alpha$ would be a good compromise, which with $2\theta_M = 120°$ would result in a match between required and available resolution within the range of 2θ up to 150° (fig. 1). For the high-resolution diffractometer with $\alpha = 0.1°/\sqrt{2}$, a value of $\beta = 2\alpha$ corresponds with the mosaic spread that can be obtained with standard squashed germanium crystals. However, if $\alpha_2 < 2\beta$, the effective mosaic spread is determined by α_2, as can readily be checked by putting $\alpha_2 = x\beta < \alpha_1 \sim \alpha_3$, and obtaining the effective mosaic spread as

$$[2x^2/(x^2+4)]^{\frac{1}{2}}\beta$$

for example, halving α_2 is equivalent to almost halving β. It would be useful then to choose a monochromator with $\beta > 2\alpha$ and to use α_2 to control the effective mosaic spread: this would make it possible to boost the line intensity, if required, for measurements near the focussing geometry.

6. Sample size, vertical divergence, and effective intensity

It is usually most convenient to use a cylindrical sample, especially if the sample is to be rotated to reduce preferred orientation. A thick planar sample produces an undesirable increase with $\cos^{-1}\theta$ of the width of the diffracted beam, assuming a θ–2θ scan is employed with the sample plane bisecting the incident and scattered rays; the neutron path length, and therefore absorption, also increases with $\cos^{-1}\theta$. In either case, absorption correction errors limit the thickness of the specimen, and a 0.5 cm to 2.0 cm diameter is usual. The height of the specimen is limited by the beam size and the vertical divergence which can be tolerated, but the latter is not a serious problem since an additional söller collimator can be used to limit vertical divergence. In practice, the beam height is usually no more than 10 cm, and with 10 cm counters at a distance of 120 cm the vertical divergence would be 5°. The use of the full height of the beam is doubly attractive, because then both the sample volume and the vertical divergence can be maximized: there is a fourfold increase in line intensity on doubling both the specimen and counter heights.

The vertical divergence must ultimately be limited because of the broadening it produces in the line width for scattering angles other than 90°. This broadening arises because of the curvature of the projection on the counter plane of the Laue powder diffraction cones. The ends of the counter intercept these cones at a slightly different angle than does the centre, and the recorded lines are broadened and unsymmetrical for small and large scattering angles. Appropriate corrections[9,1]) can be made for profile calculations, but this pseudo-defocussing effect cannot be allowed to become more important than normal defocussing.

The full width at half height of broadening due to a vertical divergence of $\delta\phi$ is, if $(180 - \frac{1}{2}\delta\phi) \gg 2\theta \gg \frac{1}{2}\delta\phi$:

$$\delta(2\theta)_v = (\tfrac{1}{4}\delta\phi)^2 |\cot 2\theta| = 0.017° |\cot 2\theta|,$$

$$\text{if } \delta\phi = 5°,$$

It is only for scattering angles smaller than $2\theta = 15°$ ($\cot 2\theta = 3.74$) that the effect of a vertical divergence of 5° becomes important. In fact, if we are most interested in the focussing region near $2\theta = 90°$, as is often the case for crystal structure work, we should use more extensive counters to increase the vertical divergence to 10° or more if we wish to obtain maximum line intensity.

The effective flux for a conventional powder diffractometer can also be increased by packing a large

number of counters and collimators in the equatorial plane. If the specimen is at most 2 cm wide, then with 0.25 cm thick side walls, 2.5 cm wide collimators can be spaced at intervals of 2.5° with the front ends forming a circle of radius 60 cm from the sample: this allows another 60 cm for the length of the fine collimators needed for a high-resolution machine. Such collimators can be fabricated using the technique of stretched metal blades developed at Petten, or, perhaps more easily, using the novel technique of shrunk paper or thermo plastic blades developed at Ispra[10]).

An array of 32 collimators and counters, covering a 2θ arc of 80°, would probably be the practical maximum if the ability to scan each counter over a large section of the diffraction pattern is to be retained. A large scanning range provides a large degree of overlap between the different counters and is useful for reducing intercounter calibration errors. Of course, if the high-angle counters are to reach low scattering angles, it must be possible to swing the counter bank back through the direction of the incident beam. There is then a reduction in efficiency, from the maximum of 32 times that for a single counter, since the low-angle counters do not collect useful data for part of the time.

7. Comparison with the PANDA diffractometer

The comparison is best made with the original single counter PANDA machine, with vertical divergence of $\sim 5°$ on which the $NH_4H_2PO_4$ data was collected[2]), although now the number of counters and the vertical divergence has been increased with corresponding gains in effective flux. The original machine had a variable take-off angle of up to $2\theta_M = 90°$, a squashed germanium monochromator of mosaic spread $\beta = 7'$ giving a wavelength of 1.54 Å from the (511) plane, $\alpha_1 = \alpha_3 = 30'$ and $\alpha_2 \simeq 30'$. The beam size permitted the use of a sample of height 5 cm by 1.5 cm diameter. According to section 5, the mosaic spread of the monochromator is far too small for this medium-resolution machine, but monochromators with larger mosaic spread were not then available.

The high-resolution machine would have $2\theta_M \simeq 120°$, a squashed germanium monochromator (533) plane giving $\lambda = 1.49$ Å with $\beta = 10'$ to $20'$, $\alpha_1 = \alpha_3 = \alpha \simeq 5'$ and $\alpha_2 = 2\beta = 20'$ to $40'$. The sample height would be 10 cm and the vertical divergence at least 5°. Because of the factor $\cos^{-2}\theta$ in the expression for the integrated reflecting power[11]), increasing the take-off angle from 90° to 120° reduces the intensity by a factor of 0.67, and a further small reduction occurs because the Debye–Waller factor is larger for (533) than for (511). These losses are compensated by the increased length of the sample. The reduction in $\alpha_1 = \alpha_3$ from $30'$ to $5'$ produces the largest reduction, by a factor of 36, in integrated line intensity, but the overall loss factor is reduced to 25 when account is taken of the increase of β from $7'$ to $10'$. This factor of 25 in integrated intensity, or 5 in peak height, together with the further factor of 8 required when the crystal cell size is doubled to 15 Å, can be obtained with the use of 32 counters and the HFR at Grenoble, which has a useful flux of up to 10 times that of the Harwell reactor. In practice, the reactor gain factor would be reduced to ~ 6, because the only suitable position is 5 m from the reactor face (D2B position). The only other possible position would be on a thermal-neutron guide, but there the reactor gain factor would fall to ~ 1 because of reduced vertical divergence and guide tube transmission losses: in this position it would be necessary to relax the resolution and to work on less complex crystal structures.

8. Alternatives to the multicounter diffractometer

We have shown that a conventional neutron powder diffractometer can be designed to give sufficient intensity for the highest resolution permitted by the particle size and extinction effects. It might seem unnecessary then to look for an alternative and less well-tried powder diffraction technique which will necessarily face the same particle size and extinction limits. However, there are at least three alternatives which appear to offer particular advantages over the conventional machine, and they deserve special mention. We will not attempt to make a detailed comparison; this is impossible in any case since the alternatives are not so well developed as the conventional diffractometer. In the final analysis, they can only be judged on published results, and as yet there are insufficient results for a complete comparison.

8.1. The position-sensitive detector

In principle, the best efficiency can be obtained from a powder diffractometer by surrounding the sample with a position-sensitive detector (PSD), so that all of the scattered radiation is collected. In practice, this is not quite so attractive, since we are only interested in the relatively small sections of the diffraction cones for which geometrical focussing is good. We might expect though, that even for these regions, in the equatorial plane, a PSD detector would be more efficient than an angle-sensitive detector such as a multi-collimator.

It is easy to show that a PSD will produce the same

Gaussian line profiles needed for profile refinement as does the söller collimator. When we scan a rectangular counter element over the rectangular projection of the sample, a triangular response results due to the folding of the two rectangles. This response is the same as the triangular response of a söller collimator, and so the two systems are equivalent. When a second triangular function, representing the collimator α_1, is also folded in, an almost Gaussian profile results, as required. The best compromise for a scanning PSD is to make the detecting elements the same width as the sample, and then the fwhm or collimation of the counter (α_3) will be the angle subtended by the sample at the detector.

Of course, the PSD becomes less attractive if it must be scanned in the same way as a collimator system, but if it remains stationary, only two or three points on the profile will be obtained. These points give the integrated line intensity, but are insufficient to define the profile, especially for a complicated pattern of overlapping reflexions. Another solution would be to reduce the distance between counter elements, but then the number of elements, already very large, produces severe calibration problems. In some cases it may be easier to scan a periodic aperture over the PSD[12]). This can be designed to produce the same results as scanning the PSD itself, but the efficiency of the device would then be halved.

There is no mechanical advantage of a scanning PSD over a multicollimator, but it remains necessary to examine their relative efficiencies. For example, the "efficiency" of our proposed 32 counter multicollimator with a resolution of 0.1° over a 2θ range of 160° say, is $32 \times 0.1/160 = 2\%$. A specimen of up to 2 cm diameter might be used. This can be compared with an efficiency of up to 100% for a PSD covering the same range. However, to obtain the same *resolution*, this detector would have to be mounted on a circle of radius $(2/0.1) \times 60$ cm $= 12$ m, compared to the ~ 1.5 m required for a multidetector.

We can only reduce the size of this huge machine if we reduce the diameter of the specimen, and hence the scattered intensity. If we require only the same intensity as for the multicollimator, we can reduce the specimen diameter by a factor of $\sqrt{(100/2)} = 7$, so that we have a specimen of diameter $2/7 = 0.3$ cm. Our PSD would then have a radius of $(0.3/0.1) \times 60 = 1.8$ m, and would not be any more "efficient" than a multicollimator of smaller size.

When we calculate the relative efficiencies taking into account the sample size, we find that the PSD is only competitive at medium or low resolution. The angular spacing between söller collimators of width D packed around the sample in an arc or radius R is D/R, and their efficiency is $\alpha_3/(D/R)$. The line intensity is proportional to the square of the diameter of the sample, which can also be D if we neglect for the moment the width of the collimator side plates. The overall efficiency of the multicollimator system is then proportional to $D^2(\alpha_3/(D/R)) = D\alpha_3 R$. The overall efficiency of a PSD of the same radius is also proportional to $D^2 = D\alpha_3 R$, since the counter collimation is $\alpha_3 = D/R$. The length of the söller collimator, and the width of its side plates and collimator blades, reduces the overall efficiency of this system by a factor of ~ 0.5, but then the counters used for a PSD are only about 50% as efficient as those used for a multicollimator system. It is reasonable then to put the overall efficiencies of both systems equal and proportional to $D\alpha_3 R$. This means that the PSD is at a disadvantage for high resolution when the sample diameter must be reduced below that which can be used with a multicollimator system.

In practice, the difficulty of calibrating the larger number of counters, and of adding together the results from all of them to obtain a pattern suitable for profile analysis, is likely to weigh heavily against a PSD, even in cases where the overall efficiencies of the two systems are comparable. Another practical disadvantage of the PSD is that it collects background from a much larger region than does the multicollimator, which sees just the small volume near the sample (fig. 5). This becomes a real problem for the PSD if, as is often the case, the sample must be placed in a furnace or cryostat.

8.2. Elastic-scattering triple-axis machine

Many of the samples contain hydrogen atoms which produce a strong "incoherent" background. This problem is more serious for powders than for single crystals, since all of the powder sample contributes to the background, but only the small fraction of the crystallites having the correct orientation contribute to the Bragg peaks. However, the peak to background ratio (P/B) increases linearly with increasing resolution as is apparent from fig. 2; the peak height is proportional to the cross-sectional area of the resolution disk, while the background is proportional to its volume which becomes small for thin disks or high resolution. Caglioti[18]) has shown that the peak-to-background ratio can also be greatly increased by using an energy-analysing crystal in front of the counter to discriminate against the "incoherent" neutrons associated with inelastic scattering. He has obtained an improvement by a factor of ~ 6 in this ratio for NH_4Br.

It is easy to show, though, that increasing P/B is in itself not sufficient to improve the data: it is instead necessary to improve the product of peak height and P/B ratio, and this Caglioti has not done, since the peak height is apparently reduced by a factor of ~ 10 when the analysing crystal is introduced. To see what is required, we need only write down the proportional error in the peak P:

$$\sigma(P)/P = (P+B)^{\frac{1}{2}}/P = \{[(P/B)+1]/P(P/B)\}^{\frac{1}{2}}.$$

We have neglected the error in subtracting the background, which will be well determined by several points in the profile, and in any case, this doesn't make any difference to our conclusions. Obviously, if $\sigma(P)/P$ is to be reduced, the product $P(P/B)$ must be increased, especially if $(P/B) \ll 1$. Unfortunately this product is reduced if an analysing crystal is used, except perhaps in the case of pyrolytic graphite analysers.

Another disadvantage of using analysing crystals is that it then becomes more difficult to have a multicollimator bank. If the product $P(P/B)$ is to be maximized, it seems better to simply increase the effective P using a multicollimator system rather than to increase (P/B) and reduce P with an analysing crystal.

8.3. The time-of-flight backscattering machine

An interesting alternative to the conventional diffractometer, where the wavelength is fixed and the scattering angle varied, is the time-of-flight (TOF) machine where the scattering angle is fixed and the wavelength varied[13]). The best example, initiated by Maier-Leibnitz, uses extreme backscattering[14]) so that, when the radius of the Ewald sphere is changed, it cuts spheres at tangents (fig. 3). This is similar to the situation with the conventional diffractometer in the focussing geometry, but with the TOF machine the high resolution is maintained for all values of $(\sin\theta/\lambda)$. As well, the intersection is practically simultaneous over a large solid angle in the backscattering direction, and wide-angle counters can be placed to collect all of this diffracted radiation. Steichele[17]) has calculated that a TOF machine would have between 3 and 20 times the effective intensity of a five-counter conventional diffractometer operating under similar conditions of high resolution, and claims that this could be increased by a further factor of 15 by the use of an extended counter array covering all of the backscattering region.

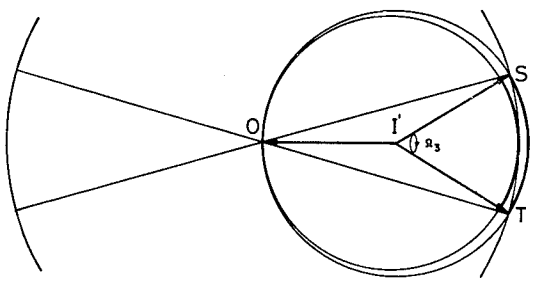

Fig. 3. Backscattering TOF geometry in reciprocal space. When the neutron wavelength is varied, the Ewald sphere ST cuts through the powder diffraction sphere at a tangent. Scattering occurs almost simultaneously for a large solid angle Ω_3 in the backscattering direction ($2\theta = 180°$), c.f. fig. 2. The line width depends on the "collimation" Ω_1 and Ω_3 of the incident and scattered beams, and on the spread in the measurement of the neutron wavelength (velocity).

This comparison is not quite correct, because the optimum combination of söller divergences has not been used to calculate the intensity of the conventional machine. If, instead of the choice of $\alpha_1 = \alpha_3 = 5'$, $\alpha_2 = 10'$, and $\beta = 7'$, the combination $\alpha_1 = \alpha_3 = 5'$, $\alpha_2 = 20'$–$40'$ and $\beta = 10'$–$20'$ is used, section 5 shows that the intensity is increased by a factor of between 3 and 11 without sacrifice of the high resolution. If 32 counters are used instead of 5, and the vertical divergence at the counter increased to 10°, the intensity for the conventional machine is increased by a further factor of ~ 12, and then compares quite well with that for the TOF machine, even when all of the backscattered neutrons are collected.

The other advantage claimed for the backscattering TOF machine is the extended range in $(\sin\theta/\lambda)$ which can be reached because $2\theta = 180°$ and wavelengths down to $\lambda = 0.6$ Å can be used. However, limiting the scattering angle to 150° with a conventional machine, instead of 180°, reduces the range in reciprocal space by only 3.5%, so any advantage comes from the use of short wavelengths. Unfortunately, neutron-guide-tube transmission losses are high for short wavelengths; it is necessary to divide the neutron spectrum into a number of energy ranges and to count for a longer period in the short-wavelength range. Similar intensity difficulties are encountered with a conventional machine operating at short wavelength, but with cooled monochromators it is possible to extend the range to compete quite favourably again with the TOF machine. There is, however, a more fundamental difficulty with working at short wavelengths on either machine: as we have seen in eq. (5), the space between peaks decreases rapidly with $(\lambda/d)^2$, and for large structures the peaks become far too crowded. even for high resolution and the profile-refinement technique.

The resolution for the TOF machine is measured by $\Delta\lambda/\lambda$, where $\Delta\lambda$ is the difference in wavelength between peaks which are just resolved. If this is to be compared

with $\Delta(2\theta)$ for the conventional diffractometer we must obtain the derivative $\partial\theta/\partial\lambda$ of the Bragg equation, from which it follows that a change $\Delta\theta$ in the Bragg angle is equivalent to a change $\Delta\lambda$ in the wavelength, or Δd in the lattice dimension, where:

$$\frac{\Delta\lambda}{\lambda} = \frac{\Delta d}{d} = \cot\theta\,\Delta\theta \qquad (11)$$

$$= 5\times10^{-4}, \quad \text{if } \theta = 60^\circ \text{ and } \Delta(2\theta) = 0.1^\circ.$$

It is in fact possible to measure the wavelength to this precision using the TOF technique, provided long (150 m) flight paths are used[14]). There is a penalty, however, in that a long flight path reduces the divergence of the incident beam far below that which could be used on a backscattering machine, with corresponding losses in intensity: a neutron guide tube must be used to limit these losses, but it is less successful for short-wavelength neutrons. The TOF technique may actually be better suited to low- and medium-resolution instruments if high intensity is required, since then short path lengths and large incident solid angles can be used. It is not even necessary to have a nuclear reactor; a particle accelerator can be used to provide the required bursts of thermal neutrons[15]).

To find the resolution function required for the TOF machine, we must obtain the derivative $(\partial d/\partial p)$ from the Bragg equation (4) and put $\Delta p = 1$ as before. Then:

$$\frac{\Delta d}{d} = \frac{1}{2\sin^2\theta}\left(\frac{\lambda}{2d}\right)^2. \qquad (12)$$

This is the same as for the conventional machine, as can be seen by combining eqs. (11) and (5). In fig. 4 we have plotted the required resolution against that available for both TOF and conventional diffractometers. The instrument parameters for the conventional machine have been chosen to obtain a good match between the required and available resolution functions, but this is not possible with the TOF machine, where $\Delta\lambda/\lambda$ increases slowly with $(\sin\theta/\lambda)$, instead of decreasing rapidly as desired. This means that the resolution of the TOF backscattering machine is much better than it need be at low $(\sin\theta/\lambda)$ and much worse at high $(\sin\theta/\lambda)$. The intensity and resolution problems make it difficult to use the extended range in $(\sin\theta/\lambda)$, except for simple structures.

The TOF backscattering geometry has some practical advantages in that only one small window is needed for both the incident and diffracted beams. This may make it easier to construct high-pressure sample containers, for example[16]). However, it has the disadvantage that everything within the path of the beam scatters into the counters, whereas with the conventional machine scattering from cryostats, furnaces, and pressure cells can be eliminated for a wide range of 2θ simply by limiting the dimensions of the incident and diffracted beams, as shown in fig. 5.

Nothing can yet be said about the precision of the TOF diffraction pattern, because data refinements have not been completed, but there are some formidable sources of possible systematic error. Steichele[17]) groups them into five sections: irregularities in the incoming spectrum, differences in the efficiencies of the counters, inhomogeneities in the intensity of the incoming beam or in the sample, measurement of the incoming spectrum, and measurement of the absorption characteristics of the sample.

In particular, it is likely that extinction will be a more serious problem for a TOF machine than for a conventional powder diffractometer. Primary extinction may become important, because long wavelengths must be

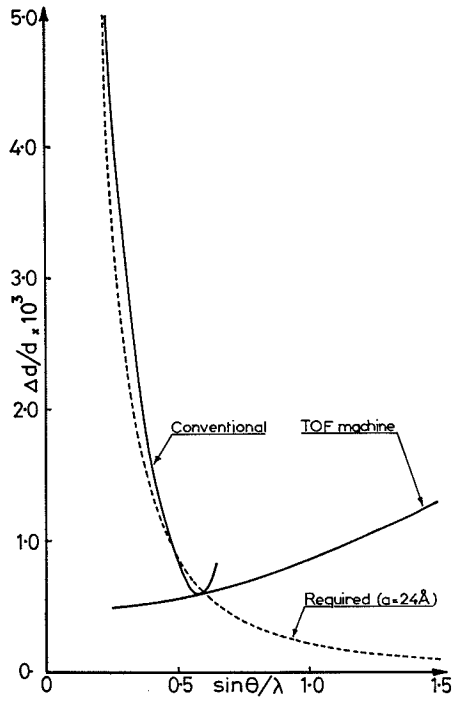

Fig. 4. Resolution functions for the conventional and backscattering TOF powder diffractometers, compared to that required to resolve adjacent lines for a cubic crystal with $a = 24$ Å. The TOF machine has higher resolution for low $(\sin\theta/\lambda)$, and lower resolution than required for high $(\sin\theta/\lambda)$. The conventional machine can be designed to match the resolution required at low and medium $(\sin\theta/\lambda)$, but the high $(\sin\theta/\lambda)$ region cannot be reached, unless the wavelength is reduced, and then the resolution again falls below that required.

used to obtain the low-order reflexions in the backscattering geometry. A secondary extinction effect also occurs with powder measurements, since a neutron reflected from one crystal grain may be reflected again by another. But with a conventional machine the probability of multiple reflexion does not depend on the structure factor, so secondary extinction does not give a systematic error as it does with single crystals: the effect is equivalent to absorption, and can be included in this correction. With a TOF machine, though, reflexions reduce particular wavelengths, giving sharp Bragg cut-offs in the spectrum of the transmitted beam: they can easily be seen on the Garching diffractometer. This produces systematic errors in the reflexions very like those produced by secondary extinction in a single crystal. However, since the orientation distribution for a powder is isotropic, secondary extinction corrections can in principle be made precisely.

In fact, it is likely that all these difficulties will be largely overcome, and that the TOF backscattering machine will eventually prove superior in some respects to the conventional diffractometer. The margin of superiority will not be very large, but there is a certain intellectual satisfaction in using this most elegant technique.

9. Conclusion

A re-examination of the conditions for optimum resolution and intensity for a conventional powder diffractometer for crystal structure refinement has shown that it is best to have a monochromator take-off angle of $\sim 120°$, $\alpha_1 = \alpha_3 = \alpha$, $\beta = 2\alpha \rightarrow 4\alpha$, $\alpha_2 = 2\beta$, and a vertical divergence at the counter of at least 5°. These conditions cannot be completely satisfied for a medium-resolution diffractometer ($\alpha \simeq 0.5°$), because monochromating crystals with large mosaic spread β are not available. To go to the highest resolution permitted by the powder particle size [$\Delta(2\theta) \simeq 0.1°$ or $\Delta d/d \simeq 10^{-3}$], it is only necessary to reduce $\alpha_1 = \alpha_3 = \alpha$, since the mosaic spread of the standard squashed germanium monochromators ($\sim 0.2°$) then satisfies the optimum conditions. The intensity then falls only with α^2 and the peak height with α; it is possible, using multiple counters on a high-flux reactor, to make up these losses and as well to provide the additional factor of eight in effective intensity required to examine structures twice as large in linear dimensions as those possible now, i.e. unit cells of up to 3500 Å^3 volume and low symmetry.

This high-resolution powder diffractometer would open up a new field in crystallography, because it would then be possible to quickly compare quite complex structures under different conditions of temperature, pressure, and chemical composition. Such a comparison can yield an insight into crystal forces and packing which is not at present available from single-crystal measurements, which are usually confined to standard temperature and pressure. As well, there are many interesting materials for which single crystals are either too small, twinned, or otherwise unsuitable for structural measurements. The powder method also has the advantage that systematic errors such as extinction are much less important than for single-crystal work, and the structural results can therefore be more precise. This is important, because the measurement of exact atomic positions and vibrational amplitudes is the first step in the study of electronic bonding using X-ray or electron-diffraction techniques. Precise structural information is also required for the study of phase transitions, which involve very small changes in the atomic positions and vibrational amplitudes.

Finally, we have examined some other techniques which might be used for neutron powder diffraction.

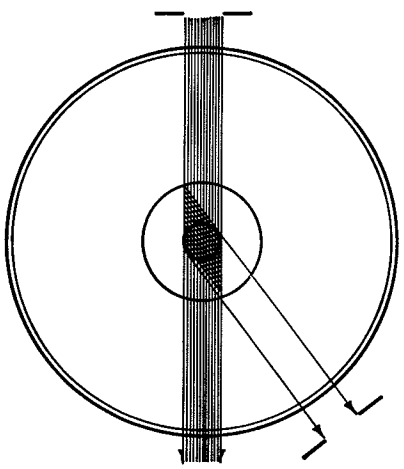

Fig. 5. The scattering volume seen by the position-sensitive detector and backscattering TOF machines (shaded) is larger than that seen by the conventional diffractometer (cross-hatched). This can be important if the sample is enclosed in a cryostat or furnace. On the other hand, with the backscattering machine one small window serves for both the incident and scattered beams.

This paper took shape at Harwell and Grenoble in late 1973 and early 1974 during discussions with Drs Bertaut, Dachs, Fender, Lomer, Rietveld, Steichele, Steiner, Wedgewood, Willis, Windsor, and others who have contributed many ideas for which the author is most grateful.

References

1) H. M. Rietveld, J. Appl. Cryst. **2** (1969) 65.

2) A. W. Hewat, Nature **246** (1973) 90.

3) A. J. C. Wilson, *Mathematical theory of X-ray powder diffractometers* (Philips Techn. Lib., Amsterdam, 1963).

4) H. P. Klug and L. E. Alexander, *X-ray diffraction procedures* (J. Wiley and Sons, New York, 1959) 2nd ed.

5) G. E. Bacon, *Neutron diffraction* (1972) 2nd ed. p. 56.

6) F. A. Wedgewood, unpublished Harwell report (1973).

7) G. Caglioti, A. Paoletti and F. P. Ricci, Nucl. Instr. **3** (1958) 223.

8) B. T. M. Willis, Acta Cryst. **13** (1960) 763.

9) Ref. 4, p. 251.

10) H. Meister and B. Weckermann, Nucl. Instr. and Meth. **108** (1973) 107.

11) W. H. Zachariasen, *X-ray diffraction in crystals* (J. Wiley and Sons, New York, 1945) equations 3.160.

12) W. Lomer, private communication.

13) K. C. Turberfield in *Thermal neutron diffraction* (ed. B. T. M. Willis; Oxford University Press, London, 1970).

14) E. Steichele and P. Arnold, Phys. Letters **44A** (1973) 165.

15) C. G. Windsor, private communication.

16) R. M. Brugger, R. B. Bennion, T. G. Worlton and E. R. Peterson, *Research applied nuclear pulsed systems* (Dubna, 18–22 July 1966; IAEA, Vienna, 1967).

17) E. Steichele in: High resolution powder diffractometers, unpublished ILL working party report (1974).

18) G. Caglioti in *Thermal neutron diffraction* (ed. B. T. M. Willis; Oxford University Press, London, 1970).